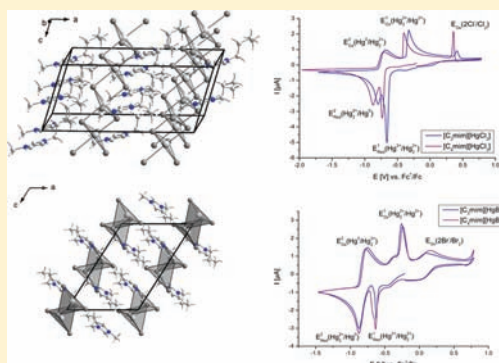


Mercuric Ionic Liquids: $[C_n\text{mim}][\text{HgX}_3]$, Where $n = 3, 4$ and $X = \text{Cl}, \text{Br}$ Bert Mallick,[†] Andreas Metlen,^{‡,§} Mark Nieuwenhuyzen,[§] Robin D. Rogers,^{*,‡,§} and Anja-Verena Mudring^{*,†,‡}[†]Anorganische Chemie I-Festkörperchemie und Materialien, Ruhr-Universität Bochum, D-44780 Bochum, Germany[‡]Department of Chemistry and Center for Green Manufacturing, The University of Alabama, Tuscaloosa, Alabama 35487, United States[§]The Queen's University Ionic Liquid Laboratories, QUILL, Queen's, University of Belfast, Belfast BT9 5AG, U.K.

Supporting Information

ABSTRACT: A series of mercury(II) ionic liquids, $[C_n\text{mim}][\text{HgX}_3]$, where $[C_n\text{mim}] = n$ -alkyl-3-methylimidazolium with $n = 3, 4$ and $X = \text{Cl}, \text{Br}$, have been synthesized following two different synthetic approaches, and structurally characterized by means of single-crystal X-ray structure analysis ($[C_3\text{mim}][\text{HgCl}_3]$ (1), Cc (No. 9), $Z = 4$, $a = 16.831(4)$ Å, $b = 10.7496(15)$ Å, $c = 7.4661(14)$ Å, $\beta = 105.97(2)^\circ$, $V = 1298.7(4)$ Å³ at 298 K; $[C_4\text{mim}][\text{HgCl}_3]$ (2), Cc (No. 9), $Z = 4$, $a = 17.3178(28)$ Å, $b = 10.7410(15)$ Å, $c = 7.4706(14)$ Å, $\beta = 105.590(13)^\circ$, $V = 1338.5(4)$ Å³ at 170 K; $[C_3\text{mim}][\text{HgBr}_3]$ (3), $P2_1/c$ (No. 14), $Z = 4$, $a = 10.2041(10)$ Å, $b = 10.7332(13)$ Å, $c = 14.5796(16)$ Å, $\beta = 122.47(2)^\circ$, $V = 1347.2(3)$ Å³ at 170 K; $[C_4\text{mim}][\text{HgBr}_3]$ (4), Cc (No. 9), $Z = 4$, $a = 17.093(3)$ Å, $b = 11.0498(14)$ Å, $c = 7.8656(12)$ Å, $\beta = 106.953(13)^\circ$, $V = 1421.1(4)$ Å³ at 170 K). Compounds 1, 2, and 4 are isostructural and are characterized by strongly elongated trigonal $[\text{HgX}_3]$ bipyramids, which are connected via common edges in chains. In contrast, 3 contains $[\text{Hg}_2\text{Br}_6]$ units formed by two edge-sharing tetrahedra. With melting points of 69.3 °C (1), 93.9 °C (2), 39.5 °C (3), and 58.3 °C (4), all compounds qualify as ionic liquids. 1, 2, and 4 solidify upon fast cooling as glasses, whereas 3 crystallizes. Cyclic voltammetry shows two separate, quasi-reversible redox processes, which can be associated with the $2\text{Hg}^{2+}/\text{Hg}_2^{2+}$ and $\text{Hg}_2^{2+}/2\text{Hg}$ redox couples.



INTRODUCTION

Complex mercuric halides have been widely studied because of their interesting and often complicated structural features, where often the formation of complex superstructures and modulated structures has been observed.¹ In that respect, complex mercuric halides with inorganic Cs^I as the counterion have been studied most extensively, and in the system $\text{Cs}^I/\text{Hg}^{II}/\text{Cl}^-$, compounds of composition Cs_3HgCl_5 ,² Cs_2HgCl_4 ,³ CsHgCl_3 ,⁴ CsHg_2Cl_5 ,⁵ and $\text{CsHg}_5\text{Cl}_{11}$ ⁶ are known and have been structurally characterized. For the $\text{Cs}^I/\text{Hg}^{II}/\text{Br}^-$ system, crystal structures of Cs_3HgBr_5 ,⁷ Cs_2HgBr_4 ,⁸ CsHgBr_3 ,^{4a,9} and CsHg_2Br_5 ¹⁰ have been determined unequivocally. Mixed halides such as CsHgCl_2Br and CsHgClBr_2 are also known.^{4a}

The structural variety of complex halogenodimercurates(II) with organic counteranions is even more diverse. Here the coordination number of 4 for Hg^{II} is by far preferred. Aside from monomers as found in bis(methylammonium)-tetrachloromercury(II),¹¹ condensed polyanions are found, for example, dimers of corner-sharing tetrahedra in *mer*-bis(diethylenediamine)cobalt(III)- $(\mu_2$ -chloro)hexachlorodimercury(II),¹² dimers of edge-sharing tetrahedra in bis(tetra-*n*-butylammonium)-bis(μ_2 -chloro)bis[dichloromercury(II)],¹³ corner-sharing trimers in bis(μ_2 -chloro)[*N,N'*-bis(2-aminoethyl)amine-*N,N'*]dicopper(II)-bis(μ_2 -chloro)octachlorotrimercury(II),¹⁴ edge-sharing trimers in bis(μ_2 -butylimido)tris(*tert*-butylimido)(*tert*-butylamido)-

dimanganese-tetrakis(μ_2 -chloro)tetrachlorotrimercury(II),¹⁵ cyclic trimers in bis(tetraethylammonium)octachlorotrimercury(II),¹⁶ tetramers in 2-chloropyridinium trichloromercury(II),¹⁷ chains of corner-sharing tetrahedra in tris(dimethylammonium)-tris(μ_2 -chloro)hexachlorotrimercury(II),¹⁸ as well as chains of edge-sharing octahedra in trimethylammonium catena(μ_2 -chloro)-dichloromercury(II).¹⁹

With such diversity in the Hg^{II} coordination of halides possible, we were interested in determining whether mercury(II) halides could be developed into a consistent, controllable class of ionic liquids (ILs) by the appropriate choice of large, asymmetric, and charge-diffuse organic cations. ILs, often defined as salts that melt below 100 °C,²⁰ have received considerable attention over the past years as a widely tunable class of solvents or materials. Many compounds belonging to this class have desirable features such as low vapor pressure, low flammability, comparatively high thermal stability, and high ionic conductivity, which render them interesting in various fields of applications.

ILs have been described as being useful for the extraction of metal ions from solvents, and in this context, hydrophobic ILs have been described as useful extractants for Hg^{II} from water.^{21–24} Also, the removal of mercury from gases using ILs has been reported.^{25,26} If at some point an IL-based process for the extraction

Received: July 6, 2011

Published: December 14, 2011

of Hg^{II} cations becomes reality, knowledge of the physicochemical properties of the resulting salts is mandatory.

In addition, metal-based ILs are of interest because they offer the additional advantage that the properties of the metal, such as, for example, magnetism,²⁷ luminescence,²⁸ or catalytic behavior²⁹ can be introduced to the liquid. A variety of metal chloride based (SnCl₂, SnCl₄, LaCl₃, YCl₃, TiCl₄, MnCl₂, FeCl₃, CoCl₂, NiCl₂, PdCl₂, PtCl₄, IrCl₄, CuCl, AgCl, AuCl₃, ZnCl₂, CdCl₂, and InCl₃) ILs, aside from the well-known AlCl₃-based systems, have already been synthesized, and some of them have been structurally characterized.³⁰

Mercury-containing ILs are not only of interest in the context of extraction and environmental chemistry but are also important for fundamental studies because mercury is, aside from gold, the element where relativistic effects in chemistry become most obvious and important.³¹ The pairing of mercury chemistry with ILs allows extension of the classical molten salt chemistry³² to the low-temperature regime. Polyatomic species³³ by comproportionation would allow for new insights into chemical bonding and how relativity affects chemistry. However, first the basics have to be explored and thus, here, we describe the syntheses and key properties of ILs comprised of complex mercury(II) halide anions and a prototypical class of IL cations, 1,3-dialkylimidazolium.

EXPERIMENTAL SECTION

General Procedures. All chemicals, unless otherwise stated, were purchased from Aldrich (Steinheim, Germany, or Dorset, U.K.) and used without further purification. The imidazolium halides were prepared by the reaction of freshly distilled 1-methylimidazole (>99%) with the respective alkyl halide, following a literature procedure.³⁴ HgCl₂ and HgBr₂ were purchased from Sigma-Aldrich (Steinheim, Germany) or Merck (99.5%, Darmstadt, Germany) and used without further purification. Water was deionized in-house above 18 MΩ cm using a Barnstead (Dubuque, IA) deionization system.

Syntheses. The target compounds can be obtained via two different synthetic approaches: (a) In an ionothermal synthesis, the respective mercuric halide is directly reacted with the desired alkylimidazolium halide at elevated temperature. The reactions were carried out under a dry nitrogen atmosphere using standard glovebox and Schlenk techniques. (b) An alternative route is classical solution chemistry where the respective imidazolium halide and the corresponding mercuric halide are reacted in water and/or ethanol.

Method a. [C_{*n*}mim][HgX₂], where *n* = 3, 4 and X = Cl, Br. HgCl₂ or HgBr₂ was added to an equimolar amount of the respective imidazolium halide in a glass tube of 12 mm inner diameter. The reaction tubes were sealed under a dynamic vacuum and heated to 130 °C in a laboratory furnace. The completion of the reaction was observed by the formation of a homogeneous, colorless liquid. To obtain single crystals of sufficient quality for single-crystal X-ray structure analysis, the reaction ampules were slowly cooled (−3 °C/h) from 130 °C to room temperature (25 °C). Quantitative yields were achieved.

[C₃mim][HgCl₃] (**1a**). Elem Anal. Calcd for C₈H₁₃N₂HgCl₃: C, 19.46; H, 3.03; N, 6.48. Found C, 19.10; H, 3.12; N, 6.40. Mp = 69.3 °C; T_g = −66.4 °C. ¹H NMR (300 MHz, water-*d*₂): δ_H 0.82 (t, *J* = 7.38 Hz, 3H), 1.76 (dt, *J* = 7.23 and 7.38 Hz, 2H), 3.77 (s, 3H), 4.02 (t, *J* = 7.23 Hz, 2H), 7.31 (s, 1H), 7.35 (s, 1H), 8.59 (s, 1H). ¹³C NMR (75 MHz, water-*d*₂): δ_C 9.8, 22.82, 35.57, 51.06, 122.16, 123.44. MIR (cm^{−1}): 3147w, 3106w, 2966w, 2933w, 2875m, 1629m, 1565s, 1461s, 1382m, 1336m, 1166s, 902m, 838s, 755s, 659m, 620s. FIR/Raman (cm^{−1}): 330w (IR/Ra), 276s (IR/Ra), 240w (IR/Ra), 100s (IR/Ra). ESI-MS (positive): 125.10097 (100), 125.5657 (50), 126.1109 (10) (C₃mim⁺); 286.2222 (20), 721.7954 (15). ESI-MS (negative): 306.8772 (100) (HgCl₃[−]), 578.7821 (10), 839.3607 (5).

[C₄mim][HgCl₃] (**2a**). Elem Anal. Calcd for C₇H₁₃N₂HgBr₃: C, 14.87; H, 2.32; N, 4.95. Found C, 14.36; H, 2.23; N, 4.61. Mp = 39.5 °C, no glass transition. ¹H NMR (300 MHz, water-*d*₂): δ_H 0.83 (t, *J* = 7.43 Hz, 3H), 1.79 (dt, *J* = 7.20 and 7.43 Hz, 2H), 3.82 (s, 3H), 4.08 (t, *J* = 7.20 Hz, 2H), 7.36 (s, 1H), 7.42 (s, 1H), 8.67 (s, 1H). ¹³C NMR (75

MHz, water-*d*₂): δ_C 10.01, 22.95, 35.87, 51.15, 122.27, 123.55, 135.92. MIR (cm^{−1}): 3143w, 3112w, 3077m, 2958w, 2927w, 2867m, 1610m, 1569s, 1465s, 1373m, 1166s, 902m, 838s, 750s, 659m, 619s. FIR/Raman (cm^{−1}): 213w (IR/Ra), 185s (IR/Ra), 135w (IR/Ra) 100w (IR/Ra). ESI-MS (positive): 125.1101 (100), 126.1137 (10) (C₃mim⁺); 160.9725 (20), 203.0161 (15), 483.5004 (10), 896.9516 (3). ESI-MS (negative): 80.9185 (100) (Br[−]); 440.7221 (40) (HgBr₃[−]).

[C₃mim][HgBr₃] (**3a**). Elem Anal. Calcd for C₈H₁₃N₂HgCl₃: C, 21.54; H, 3.39; N, 6.28. Found C, 21.50; H, 3.10; N, 6.22. Mp = 93.9 °C; T_g = −60.5 °C. ¹H NMR (300 MHz, water-*d*₂): δ_H 0.79 (t, *J* = 7.60 Hz, 3H), 1.19 (dt, *J* = 7.18 and 7.60 Hz, 2H), 1.72 (quin, *J* = 7.18 Hz, 2H), 3.76 (s, 3H), 4.07 (t, *J* = 7.18 Hz, 2H), 7.30 (s, 1H), 7.34 (s, 1H), 8.58 (s, 1H). ¹³C NMR (75 MHz, water-*d*₂): δ_C 12.5, 18.7, 31.2, 35.5, 49.2, 122.2, 123.4, 135.8. MIR (cm^{−1}): 3147m, 3106s, 3091w, 2966m, 2933s, 2877w, 1623m, 1565s, 1461m, 1168s, 840s, 754s, 657w, 622s. FIR/Raman (cm^{−1}): 330w (IR/Ra), 273s (IR/Ra), 230w (IR/Ra), 100s (IR/Ra). ESI-MS (positive): 139.1251 (100), 140.1274 (10) (C₄mim⁺); 313.2153 (5); 759.2126 (3). ESI-MS (negative): 306.8774 (100) (HgCl₃[−]); 383.1560 (10); 559.2452 (10); 578.7863 (5); 733.3352 (10); 907.4290 (10); 1083.5248 (10); 1257.6204 (10); 1431.7177 (10).

[C₄mim][HgBr₃] (**4a**). Elem Anal. Calcd for C₈H₁₃N₂HgBr₃: C, 16.58; H, 2.61; N, 4.83. Found C, 16.77; H, 2.61; N, 4.89. Mp = 58.3 °C; T_g = −73.2 °C. ¹H NMR (300 MHz, water-*d*₂): δ_H 0.79 (t, *J* = 7.39 Hz, 3H), 1.19 (dt, *J* = 7.23 and 7.62 Hz, 2H), 1.72 (quin, *J* = 7.23 Hz, 2H), 3.76 (s, 3H), 4.07 (t, *J* = 7.23 Hz, 2H), 7.29 (s, 1H), 7.35 (s, 1H), 8.58 (s, 1H). ¹³C NMR (75 MHz, water-*d*₂): δ_C 12.6, 18.7, 31.2, 35.6, 49.2, 122.2, 123.4, 135.8. MIR (cm^{−1}): 3143m, 3104s, 3089w, 2962m, 2931s, 2873w, 1618m, 1564s, 1459m, 1166s, 836s, 752s, 657w, 620s. FIR/Raman (cm^{−1}): 280w (IR/Ra), 180s (IR), 170s (Ra), 96w (Ra), 71w (IR). ESI-MS (positive): 139.1253 (100), 140.1289 (10) (C₄mim⁺); 419.0046 (5). ESI-MS (negative): 80.9185 (100) (Br[−]); 440.7221 (40) (HgBr₃[−]).

Method b. [C₄mim][HgCl₃] (**2b**). Equimolar amounts of 1-butyl-3-methylimidazolium chloride and mercuric chloride were dissolved in deionized water. After the solutions were mixed, water was allowed to evaporate isothermally under ambient conditions. Colorless crystals of the target compounds were obtained after the bulk solvent evaporated with an estimated yield of ~100%. Elem Anal. Calcd for C₈H₁₃N₂HgCl₃: C, 21.54; H, 3.39; N, 6.28. Found C, 21.68; H, 3.30; N, 5.78. ¹H NMR (500 MHz, DMSO-*d*₆): δ_H 0.90 (t, *J* = 7.36 Hz, 3H), 1.25 (dt, *J* = 7.43 Hz, 2H), 1.76 (quin, *J* = 7.33 Hz, 2H), 3.85 (s, 3H), 4.16 (t, *J* = 7.17 Hz, 2H), 7.70 (s, 1H), 7.77 (s, 1H), 9.10 (s, 1H). ¹³C NMR (75 MHz, DMSO-*d*₆): δ_C (ppm) 13.27, 18.75, 31.33, 35.77, 48.49, 122.24, 123.59, 136.44. MIR (cm^{−1}): 3152w, 3108m, 3093m, 2967w, 2937w, 2882w, 2868w, 1627w, 1573m, 1566m, 1463m, 1167s, 840m, 756m, 657m.

[C₄mim][HgBr₃] (**4b**). A total of 1.00 mmol of each [C₄mim]Br and HgBr₂ was dissolved in separate aliquots of 100 mL of EtOH. Both solutions were mixed and allowed to evaporate at room temperature. Overnight, a colorless crystalline mass formed in a yield of 28% as nearly spherical colorless particles. Elem Anal. Calcd for C₈H₁₃N₂HgBr₃: C, 16.58; H, 2.61; N, 4.83. Found C, 16.74; H, 2.83; N, 4.61. ¹H NMR (500 MHz, DMSO-*d*₆): δ_H 0.90 (t, *J* = 7.26 Hz, 3H), 1.25 (dt, *J* = 7.39 Hz, 2H), 1.76 (quin, *J* = 7.34 Hz, 2H), 3.85 (s, 3H), 4.16 (t, *J* = 7.26 Hz, 2H), 7.70 (s, 1H), 7.77 (s, 1H), 9.10 (s, 1H). ¹³C NMR (75 MHz, DMSO-*d*₆): δ_C 13.27, 18.78, 31.35, 35.77, 48.50, 122.27, 123.63, 136.46. MIR (cm^{−1}): 3167w, 3143w, 3111w, 2956m, 2930m, 2870w, 1604w, 1560m, 1457m, 1155s, 818m, 810m, 744s, 739s, 695m.

Nuclear Magnetic Resonance (NMR). NMR spectra of compounds prepared according to method a were recorded in water-*d*₂ at 25 °C on a 300 MHz Bruker (Karlsruhe, D) Avance II 300 spectrometer, with the solvent as the internal standard, or according to method b in DMSO-*d*₆ at 25 °C on a 500 MHz Bruker (Billerica, MA) AX500 spectrometer, with the solvent as the internal standard.

Differential Scanning Calorimetry (DSC). DSC scans were recorded on a Netzsch DSC 204 F1 Phoenix thermoanalyzer in silica crucibles with a heating rate of 5 °C/min. An empty sample container of the same type was used as the reference, and the thermal cycles were repeated twice.

Vibrational Spectroscopy. IR spectra were recorded as neat samples either (method a) on a IFS-66 V-S Fourier transform IR (FTIR) spectrometer or (method b) on a Perkin-Elmer (Dublin, Ireland) Spectrum 100 FTIR spectrometer. The samples were ground to a fine

Table 1. Single-Crystal Data Collection and Structure Refinement Parameters

	[C ₃ mim][HgCl ₃] (1a)	[C ₄ mim][HgCl ₃] (2a)	[C ₃ mim][HgBr ₃] (3a)	[C ₄ mim][HgBr ₃] (4a)
empirical formula	C ₇ H ₁₃ N ₂ HgCl ₃	C ₈ H ₁₅ N ₂ HgCl ₃	C ₇ H ₁₃ N ₂ HgBr ₃	C ₈ H ₁₅ N ₂ HgBr ₃
molecular mass (g/mol)	432.14	446.2	565.49	579.52
temperature (K)	298(2)	170(2)	170(2)	170(2)
wavelength (Å)	0.710 73	0.710 73	0.710 73	0.710 73
cryst syst	monoclinic	monoclinic	monoclinic	monoclinic
space group	Cc (No. 9)	Cc (No. 9)	P2 ₁ /c (No. 14)	Cc (No. 9)
unit cell dimensions				
<i>a</i> (Å)	16.831(4)	17.3178(28)	10.2043(10)	17.093 (3)
<i>b</i> (Å)	10.7496(15)	10.7410(15)	10.7332(13)	11.0498(14)
<i>c</i> (Å)	7.4661(14)	7.4706(13)	14.5796(16)	7.8656(12)
α (deg)	90	90	90	90
β (deg)	105.97(2)	105.590(13)	122.47(2)	106.953(13)
γ (deg)	90	90	90	90
volume (Å ³)	1298.7(4)	1338.5(4)	1347.2(3)	1421.1(4)
<i>Z</i>	4	4	4	4
density (calcd, kg/m ³)	2.210	2.214	2.788	2.709
abs coeff (mm ⁻¹)	12.43	12.07	20.29	19.24
<i>F</i> (000)	800.0	831.8	1016.0	1048.0
θ range for data collection	2.5–25°	2.3–25°	2.5–25°	2.2–25°
index ranges	–19 ≤ <i>h</i> ≤ 19 –12 ≤ <i>k</i> ≤ 12 –8 ≤ <i>l</i> ≤ 8	–20 ≤ <i>h</i> ≤ 20 –12 ≤ <i>k</i> ≤ 12 –8 ≤ <i>l</i> ≤ 8	–11 ≤ <i>h</i> ≤ 12 –12 ≤ <i>k</i> ≤ 12 –17 ≤ <i>l</i> ≤ 17	–20 ≤ <i>h</i> ≤ 20 –13 ≤ <i>k</i> ≤ 13 –9 ≤ <i>l</i> ≤ 9
reflns collected	3755	4381	8716	4118
indep reflns	2231 (<i>R</i> _{int} = 0.095)	2368 (<i>R</i> _{int} = 0.052)	2308 (<i>R</i> _{int} = 0.054)	2375 (<i>R</i> _{int} = 0.059)
refinement method		full-matrix least squares on <i>F</i> ²		
data/restraints/param	2231/2/121	2368/2/130	2308/0/121	2375/2/130
GOF on <i>F</i> ²	0.859	1.036	0.857	1.174
final <i>R</i> indices [<i>I</i> > 2σ(<i>I</i>)] ^a	<i>R</i> ₁ = 0.0527, <i>wR</i> ₂ = 0.1193	<i>R</i> ₁ = 0.035, <i>wR</i> ₂ = 0.089	<i>R</i> ₁ = 0.025, <i>wR</i> ₂ = 0.043	<i>R</i> ₁ = 0.055, <i>wR</i> ₂ = 0.164
<i>R</i> indices (all data) ^a	<i>R</i> ₁ = 0.0869, <i>wR</i> ₂ = 0.1280	<i>R</i> ₁ = 0.040, <i>wR</i> ₂ = 0.090	<i>R</i> ₁ = 0.044, <i>wR</i> ₂ = 0.045	<i>R</i> ₁ = 0.061, <i>wR</i> ₂ = 0.170
largest diff peak and hole (e/Å ³)	1.89 and –1.80	0.82 and –0.93	0.71 and –0.84	2.73 and –1.59
absolute structure parameter	–0.004(20)	–0.03(2)		0.03(2)

$$^a R_w(F^2) = \left\{ \sum w[(F_o^2) - (F_c^2)]^2 / \sum w[(F_o^2)^2]^{1/2} \right\}; R(F) = \sum ||F_o| - |F_c|| / \sum |F_o|.$$

powder and pressed in a KBr (MIR region) or a polyethylene matrix (FIR region). Raman spectra were measured (method a) with a FRA 106-S Fourier transform Raman spectrometer. The samples were ground to a fine powder and sealed in glass capillaries with an inner diameter of 1 mm and a wall thickness of 0.15 mm. For samples prepared according to synthesis route (b), Raman spectra were recorded on a microscope slide with a Raman Station 400F Raman spectrometer (Perkin-Elmer).

Elemental Analysis. Elemental analyses for **1a–4a** were carried out on a HEKA Tech Euro EA 3000 elemental analyzer. Compounds **2b** and **4b** were analyzed using a Perkin-Elmer 2400 series II CHNS/O elemental analyzer (Shelton, CT).

Electrospray Ionization Mass Spectrometry (ESI-MS). ESI-MS was performed on an LCT Premier from Waters using an Advion nanomate injection system (Manchester, U.K.).

Cyclic Voltammetry (CV). The experimental CV curves were obtained with a micro Autolab type III (Eco Chemie BV, Utrecht, The Netherlands). The working electrode was a platinum electrode with a surface area of 3.142 mm². As the reference electrode, a glassy carbon electrode was used. The CV experiments were carried out in a 0.025 M solution of the mercury containing ILs in 1-butyl-3-methylimidazolium bis(trifluorosulfonyl)amide ([C₄mim][Tf₂N]) and referenced to ferrocene/ferrocenium (Fc/Fc⁺) in [C₄mim][Tf₂N]. Scans were swept cathodically from the initial potential –0.2135 V vs Fc/Fc⁺ at a scan rate of 10 mV/s.

Powder X-ray Diffraction (PXRD). PXRD data were obtained to check for phase purity on an Image Plate Guinier Camera (Huber G670) diffractometer (Mo K α ; see the Supporting Information).

Crystal Structure Determinations. A few crystals of **1a**, **2a**, **3a**, and **4a** were selected and sealed in thin-walled glass capillaries of 0.3–0.5 mm outer diameter and checked by Laue photographs for their quality.

The best specimen of each compound was used to collect a complete intensity data set with the aid of a single-crystal X-ray diffractometer [Stoe IPDS II using graphite-monochromated Mo K α X-ray radiation (λ = 0.701 73 Å)]. Essential experimental conditions and resulting crystallographic data are summarized in Table 1. Further information is given as Supporting Information and can be downloaded from the web.

Data reduction with the program *X-Red*³⁵ in all cases included corrections for background, Lorentz, and polarization effects. A numerical absorption correction with the programs *X-Red*/*X-Shape*³⁶ was undertaken after optimization of the habits of the crystal. The structures were solved by direct methods with the program *SHELXS-97*.³⁷ The atoms were refined anisotropically against *F*² by a full-matrix least-squares procedure using the program *SHELXL-97*. All non-hydrogen atoms were refined anisotropically. Hydrogen atoms were constrained to ride on their respective parent atoms. Structure factors were taken from *International Tables for Crystallography*.³⁸ For crystal structure drawings, the program *Diamond* was used.³⁹

RESULTS AND DISCUSSION

Crystal Structures. **1**, **2**, and **4** are essentially isostructural and crystallize in the acentric space group Cc (No. 9) with four formula units per unit cell. To check for the absence of an inversion center, structure solution in the corresponding centric space group C2/c was attempted. However, no satisfactory solutions could be found. In contrast, **3** crystallizes in the centrosymmetric space group P2₁/c (No. 14) with four formula units per unit cell.

1, **2**, and **4** feature a planar HgX₃[–] anionic unit that is close to ideal C_{3v} symmetry. The mean Hg–X interatomic distances within the trigonal-planar unit of 2.43(8) Å (**1**-Cl), 2.44(4) Å (**2**-Cl), and 2.56(3) Å (**4**-Br) (Table 2) are about 4–7% larger

Table 2. Selected Interatomic Distances and Angles for $[C_n\text{mim}][\text{HgX}_3]$, Where $n = 3, 4$ and $X = \text{Cl}, \text{Br}$

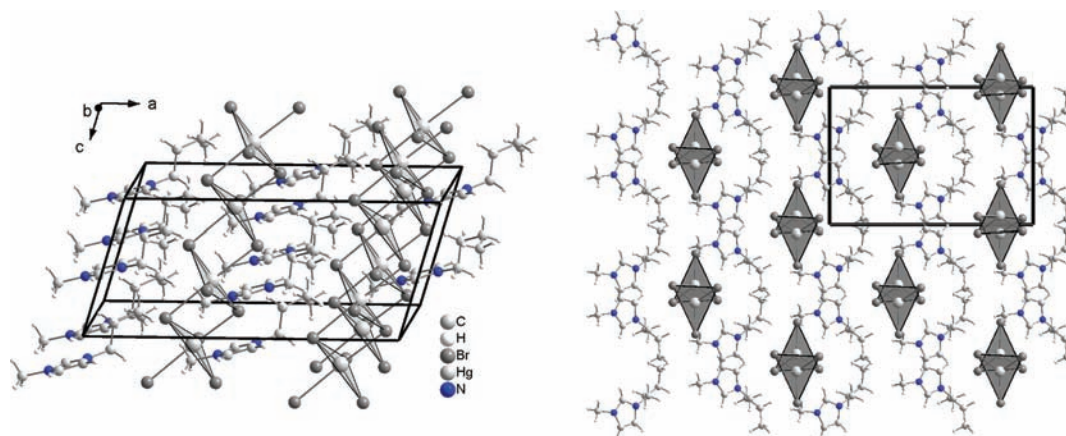
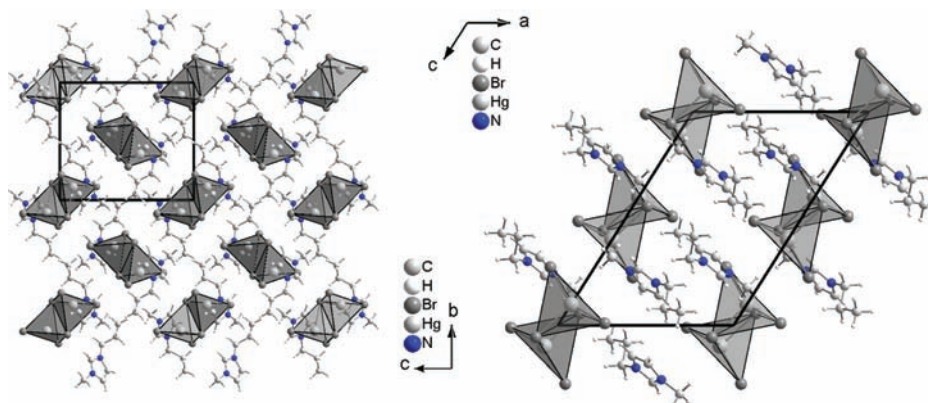
	$d/\text{\AA}$		angle/deg
[C ₃ mim][HgCl ₃] (1)			
Hg–Cl3	2.38(2)	Cl3–Hg–Cl2	112.2(2)
Hg–Cl1	2.384(5)	Cl2–Hg–Cl1	112.8(2)
Hg–Cl2	2.514(3)	Cl1–Hg–Cl3	134.0(3)
Hg–Cl2	2.86(2)		
Hg–Cl3	3.25(3)		
[C ₄ mim][HgCl ₃] (2)			
Hg–Cl2	2.412(3)	Cl2–Hg–Cl3	125.8(2)
Hg–Cl3	2.42(3)	Cl2–Hg–Cl1	114.4(2)
Hg–Cl1	2.49(2)	Cl3–Hg–Cl1	119.7(2)
Hg–Cl1	2.96(2)		
Hg–Cl3	3.02(2)		
[C ₃ mim][HgBr ₃] (3)			
Hg–Br2	2.489(8)	Br1–Hg–Br3	103.12(2)
Hg–Br3	2.49(1)	Br3–Hg–Br1	105.15(3)
Hg–Br1	2.794(1)	Br1–Hg–Br2	102.91(2)
Hg–Br1	2.807(4)	Br2–Hg–Br1	103.12(3)
[C ₄ mim][HgBr ₃] (4)			
Hg–Br1	2.537(2)	Br2–Hg–Br1	125.42(7)
Hg–Br2	2.54(2)	Br1–Hg–Br3	115.24(7)
Hg–Br3	2.59(2)	Br3–Hg–Br2	119.23(8)
Hg–Br3	3.14(2)		
Hg–Br2	3.25(2)		

than those in mercuric halide with linear X–Hg–X moieties.⁴⁰ These trigonal-planar HgX_3^- units are joined to a polymeric

chain along the crystallographic c axis, by two long X...Hg interactions, forming the axial sites in an overall trigonal-bipyramidal structure around Hg^{II}. A similar arrangement was observed, e.g., in $[\text{SMe}_3][\text{HgI}_3]$.⁴¹ These bipyramids are connected via their shortest edge to linear chains along $[001]$ (Figure 1, left). The chains are separated by imidazolium cations, as shown in Figure 1, right.

In contrast to 1, 2, and 4, compound 3 features $[\text{Hg}_2\text{Br}_6]^{2-}$ units as the anionic building units (Figure 2). They are made up of two edge-sharing $[\text{HgBr}_2\text{Br}_{2/2}]$ tetrahedra as in $[\text{H}(\text{AsPh}_3\text{O})_2][\text{Hg}_2\text{Br}_6]$.⁴² As expected, the bridging Hg–Br interatomic distances are somewhat larger [$\sim 2.800(9)$ Å] than the terminal ones [2.489(1) Å].

Angles and interatomic distances found in the imidazolium cations of 1–4 are all in the expected range.⁴³ However, some notable differences in the relative conformations are observed. The imidazolium head groups are planar, as expected, and the differences occur in the alkyl chain. The alkyl chains form angles of 102.2(2)° (1), 111.4(1)° (3), 113.4(5)° (2), and 109.1(2)° (4) with respect to the planar imidazolium head group (Figure 3). The orientation of the propyl side chain in 1 and 3 with respect to the planar imidazolium core deviates. Within the propyl side chain only, trans conformations along the C–C bonds are observed. While the relative orientation in the two butyl compounds, 2 and 4, is the same, the conformation of the side chains is different. The butyl side chain in 2 also adopts an all-anti conformation (as observed for the propyl compounds). In contrast, the substituents in 4 are arranged anti (along C5–C6) and gauche (along C6–C7).

**Figure 1.** Views of the crystal structure of 4 down $[010]$ (left) and $[001]$ (right).**Figure 2.** Views of the crystal structure of 3 down $[100]$ (left) and $[010]$ (right).

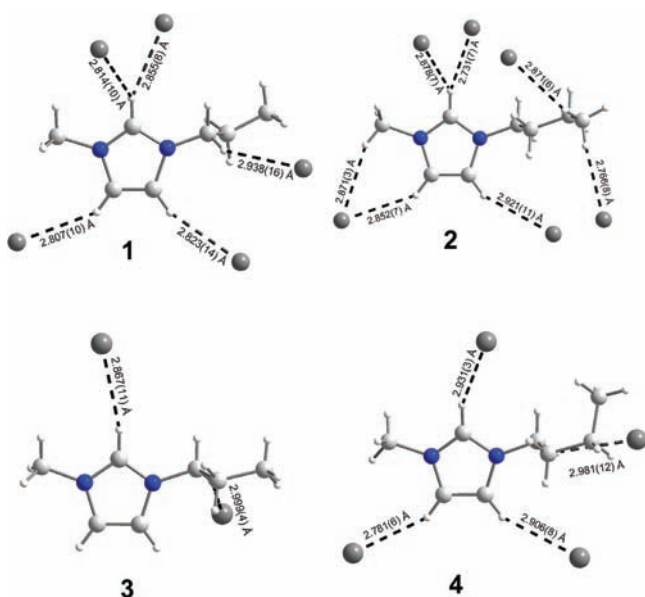


Figure 3. Cation conformations and hydrogen-bonding interactions in 1–4.

Typically, an all-anti arrangement in the alkyl side chain is energetically favored. Because there is no phase transition observed for **4** (see below), it is assumed that packing effects lead to an anti-gauche conformation of the butyl side chain in **4** in order to allow for an efficient arrangement of the $^1_\infty[\text{HgX}_3]$ polymeric strands with the cation (see the Supporting Information). Hydrogen bonding can be ruled out as the origin of the two conformations of the butyl cation in **2** and **4**, as can be seen from Figure 3.

Hydrogen bonding in 1–4 is quite weak when judged on the basis of accepted interatomic values.⁴⁴ Hydrogen-acceptor distances can be read from Figure 3. (For hydrogen-bonding interactions drawn from the perspective of the anion, see the

Supporting Information.) Because the hydrogen atoms have been computed in idealized positions in idealized positions distances might be more suitable (see the Supporting Information for a compilation). Obviously, the most acidic proton of the imidazolium ring (2-H) is engaged in all three compounds in hydrogen bonding; the less acidic protons in the 4 and 5 positions of the imidazolium ring participate in hydrogen bonding in the case of **1**, **2**, and **4**, which contain $^1_\infty[\text{HgX}_3]$ polymeric strands. However, in **3** with the $[\text{Hg}_2\text{Br}_6]^{2-}$ anion, such an interaction is not observed. Some of the alkyl side-chain protons are involved in extremely weak hydrogen-bonding interactions.

IR and Raman Spectroscopy. The FIR/Raman spectra of compounds **1** and **2** are dominated by the asymmetric Hg–Cl stretching vibrations at wave numbers of $\sim 275\text{ cm}^{-1}$ (Figure 4). In the spectra of the isostructural bromide **4**, the symmetric Hg–Br stretching vibration is observed at 170 cm^{-1} and the asymmetric one at about 180 cm^{-1} . This corresponds with the Hg–Br stretching of the terminal bromides (Figure 4). In **3** with the dimeric $[\text{Hg}_2\text{Br}_6]^{2-}$, which consists of two edge-sharing tetrahedra, the symmetric Hg–Br vibration involving the terminal bromide is observed at 185 cm^{-1} and the asymmetric one at 213 cm^{-1} (Figure 4). The peak at 135 cm^{-1} corresponds to the symmetric Hg–Br vibration involving the bridging bromide. This is in good agreement with observations for other complex mercury(II) halides with similar anions.⁴⁵ $\delta(\text{X–Hg–X})$ below 100 cm^{-1} have been associated with deformation vibrations of the complex anions and may overlap between the stretching vibrations belonging to the weaker Hg–X contacts.

ESI-MS. ESI-MS of 1–4 reveals some interesting trends. In the case of the chloride ILs **1** and **2**, no free chloride is detected in the negative mode, while bromide is found in the spectra of all bromide-containing mercuric ILs. In all cases, $[\text{HgX}_3]^-$ anions could be detected but no higher aggregates. Neither a molecular peak nor substantial clustering was observed.

Thermal Investigations. Compounds 1–4 formally belong to the class of ILs because the melting point of the crystalline

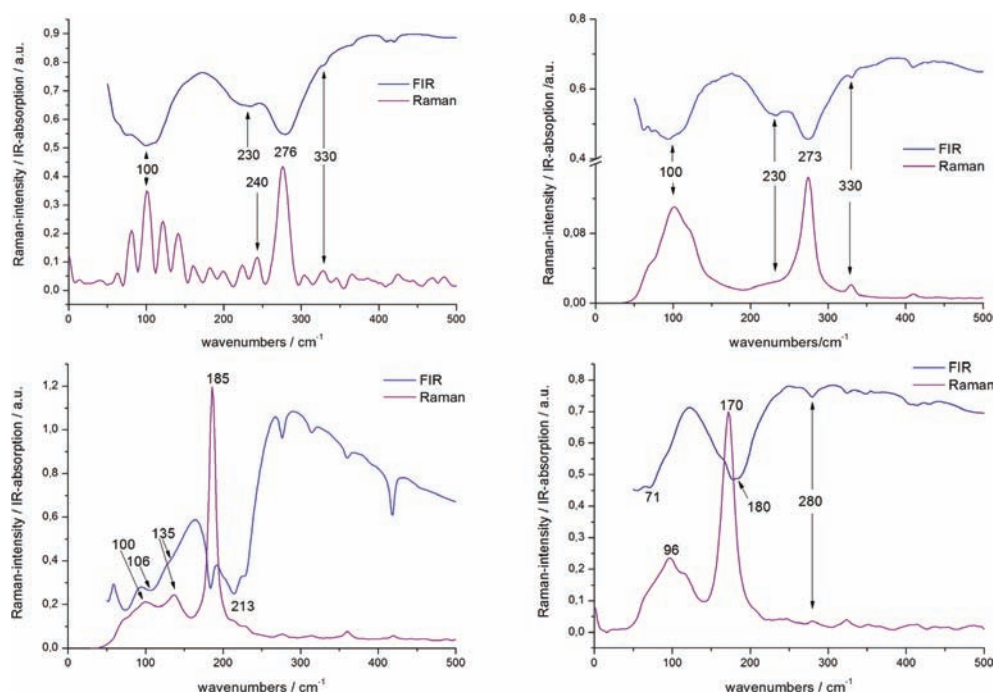


Figure 4. FIR (blue) and Raman spectra (purple) of **1** (top left), **2** (top right), **3** (bottom, left), and **4** (bottom, right).

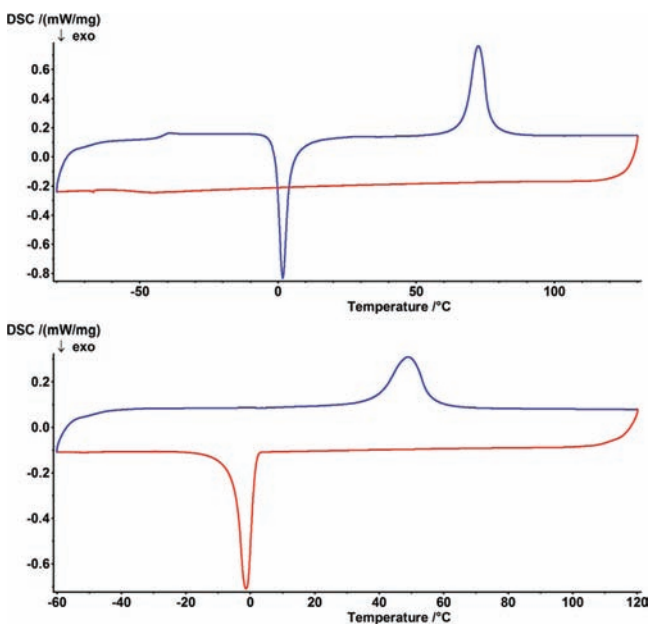
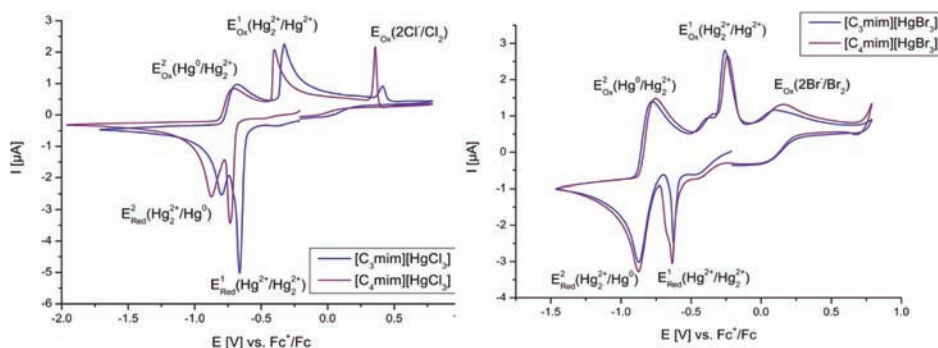
Table 3. Compiled Thermal Data (°C) for Compounds 1–4

		1	2	3	4
1st heating	melting	69.3	93.9	39.5	58.3
1st cooling	glass transition	–66.4	–60.5		–73.2
	crystallization			1.7	
2nd heating	glass transition	–43.7	–45.1		–52.2
	crystallization	–0.9	–8.4		–5.2
	melting	67.3	92.1	40.9	56.8

material is below 100 °C. The isostructural compounds **1**, **2**, and **4** show similar thermal behavior (Table 3). The DSC thermogram of **1** is given in Figure 5, top. As a typical example, for the thermograms of **2** and **4**, see the Supporting Information.

Upon cooling from the melt, the formation of a supercooled liquid over a wide temperature range is observed until solidification as a glass occurs. Recrystallization to a crystalline material sets in upon heating. This thermal behavior is commonly found for ILs.⁴⁶ However, upon extremely slow cooling (<3 °C/h), crystallization is observed. The melting point decreases upon going from a propyl to a butyl side chain on the imidazolium cation and is less for bromides compared to chlorides of the same composition.

The thermal behavior of **3** is different (Figure 5, bottom) insofar as crystallization occurs directly upon cooling from the

Figure 5. DSC thermograms of **1** (top) and **3** (bottom).Figure 6. Cyclic voltammograms of a 0.025 M solution of **1** and **2** (left) and **3** and **4** (right) in [C₄mim][Tf₂N] at 25 °C with a scan rate of 10 mV/s.

melt and no glass formation takes place. Furthermore, the temperature range where the supercooled liquid can be maintained is about 40 °C. This is significantly less than that for the other compounds. It seems that it is easy for compound **3**, which contains isolated [Hg₂Br₆]²⁻ polyanionic units, to crystallize compared to **1**, **2**, and **4**, which feature trigonal-planar HgX₃⁻ that are joined to a polymeric chain by two long X...Hg interactions.

Electrochemistry. CV shows for all mercury(II) ILs a two-step electron-transfer mechanism (Figure 6). Upon sweeping to negative voltage, one-electron reduction of Hg²⁺ to Hg²⁺ is observed first, followed by one-electron reduction of Hg^I to Hg⁰. When the potential is reversed, the respective oxidation steps are observed. However, the oxidation and reduction steps are too far apart to qualify for a reversible electrochemical reaction. It seems that both the IL cation and the halide of the complex anion have an influence on the measured half-wave potentials (Table 4).

Table 4. Compiled Electrochemical Data for Compounds 1–4

electrochemical potential (V)	[C ₂ mim][HgCl ₃] (1)	[C ₄ mim][HgCl ₃] (2)	[C ₂ mim][HgBr ₃] (3)	[C ₄ mim][HgBr ₃] (4)
$E_{\text{Ox}}^1(\text{Hg}_2^{2+}/\text{Hg}_2^{2+})$	–0.3292	–0.3999	–0.2417	–0.2608
$E_{\text{Red}}^1(\text{Hg}_2^{2+}/\text{Hg}_2^{2+})$	–0.6612	–0.7374	–0.6337	–0.6245
$E_{1/2}^1$	–0.4952	–0.56865	–0.4377	–0.44265
ΔE^1	0.332	0.3375	0.392	0.3637
$E_{\text{Ox}}^2(\text{Hg}^0/\text{Hg}_2^{2+})$	–0.6783	–0.7024	–0.752	–0.7784
$E_{\text{Red}}^2(\text{Hg}_2^{2+}/\text{Hg}^0)$	–0.7979	–0.8769	–0.8751	–0.8736
$E_{1/2}^2$	–0.7381	–0.78965	–0.81355	–0.826
ΔE^2	0.1196	0.1745	0.1231	0.0952
$E_{\text{Ox}}(\text{X}^-/\text{X}_2)$	0.413	0.357	0.1549	0.098

Changing the IL cation from C₃mim⁺ to C₄mim⁺ results in a shift of the half-wave potentials for both the Hg^{II}/Hg^I and Hg^I/Hg⁰ redox couples to more negative values. The half-wave potentials for the Hg^{II}/Hg^I redox pair are found at more negative values for the chloride ILs compared to the bromide ILs. This is in contrast to the Hg^I/Hg⁰ redox couple, where the trend is reversed. The difference between the Hg^{II}/Hg^I and Hg^I/Hg⁰ redox couples in all ILs is larger than that in aqueous solutions, and in both cases, Hg^I and Hg⁰ are less noble in the IL than in water.⁴⁷

CONCLUSIONS

We have shown that mercury-containing ILs are easily accessible via two different synthetic routes. They can be prepared using either classic solution chemistry or ionothermal/flux methods. **1**, **2**, and **4** were found to crystallize isostructurally.

They feature trigonal-planar HgX_3 units, which are connected to a chain in such a way that a trigonal-bipyramidal coordination environment is achieved for Hg^{II} in these structures. The bipyramids are connected via common edges to polymeric chains. In contrast, **3** contains isolated $[\text{Hg}_2\text{Br}_6]^{2-}$ units. These are built up by two edge-sharing $[\text{HgBr}_4]^{2-}$ tetrahedra. This is a structure unit commonly found in halomercurates(II) with large organic cations. Vibrational spectroscopy confirms the crystal structures.

The structural differences between **1**, **2**, and **4** and **3** are mirrored in their thermal behavior. Albeit, all compounds qualify as ILs, as they melt below 100 °C, **1**, **2**, and **4** solidify at moderate to fast cooling rates only as glasses. Upon heating, crystallization is observed before the compounds melt. Apparently, the formation of a polymeric anion chain of trigonal-planar HgX_3^- units, which are connected by two long $\text{X}\cdots\text{Hg}$ interactions, is quite difficult and takes sampling time in configurational space. In contrast, **3**, which features isolated $[\text{Hg}_2\text{Br}_6]^{2-}$ units, crystallizes upon cooling from the melt. Nevertheless, a strong degree of supercooling (~ 40 °C at 5 °C/min) is observed.

CV reveals two separate redox processes belonging to the $2\text{Hg}^{2+}/\text{Hg}_2^{2+}$ and $\text{Hg}_2^{2+}/2\text{Hg}$ redox couples. The measured half-wave potentials indicate that mercury behaves less noble in the IL than in water.

■ ASSOCIATED CONTENT

■ Supporting Information

X-ray crystallographic data in CIF format, powder X-ray diffraction analyses, and thermal investigations. This material is available free of charge via the Internet at <http://pubs.acs.org>.

■ AUTHOR INFORMATION

Corresponding Author

*E-mail: anja.mudring@rub.de (A.-V.M.), rdrogers@as.ua.edu (R.D.R.).

■ ACKNOWLEDGMENTS

A.-V.M. thanks the BMBF, Fonds der Chemischen Industrie (Dozentenstipendium), and the Deutsche Forschungsgemeinschaft (SPP 1191 Ionic Liquids) for generous financial support.

■ REFERENCES

- (1) House, D. A.; Robinson, W. T.; McKee, V. *Coord. Chem. Rev.* **1994**, *135/136*, 533.
- (2) Clegg, W.; Brown, M. L.; Wilson, L. J. A. *Acta Crystallogr., Sect. B* **1976**, *32*, 1968.
- (3) (a) Linde, S. A.; Mikhailova, A. Ya.; Pakhomov, V. I.; Kirilenko, V. V.; Shulga, V. G. *Koord. Khim.* **1983**, *9*, 998. (b) Bagautdinov, B.; Luedecke, J.; Schneider, M.; van Smaalen, S. *Acta Crystallogr., Sect. B* **1998**, *54*, 626. (c) Pakhomov, V. I.; Goryunov, A. V.; Ivanova-Korfini, I. N.; Boguslavskii, A. A.; Lotfullin, R. Sh. *Zh. Neorg. Khim.* **1992**, *37*, 526. (d) Pakhomov, V. I.; Goryunov, A. V.; Gladkii, V. V.; Ivanova-Korfini, I. N.; Kallaev, S. N. *Zh. Neorg. Khim.* **1992**, *37*, 1447. (e) Bagautdinov, B.; Pilz, K.; Luedecke, J.; van Smaalen, S. *Acta Crystallogr., Sect. B* **1999**, *55*, 886. (f) Bagautdinov, B.; Jobst, A.; Luedecke, J.; van Smaalen, S.; Walha, S.; Savariault, J. M.; Jaud, J.; Ben Salah, A. *Phys. Chem. News* **2002**, *8*, 69. (g) van Smaalen, S. *Acta Crystallogr., Sect. B* **2001**, *57*, 231.
- (4) (a) Natta, G.; Passerini, L. *Gazz. Chim. Ital.* **1928**, *58*, 472. (b) Zvonkova, Z. V.; Samodurova, V. V.; Vorontsova, L. G. *Dokl. Akad. Nauk SSSR* **1955**, *102*, 1115. (c) Pakhomov, V. I.; Goryunov, A. V. *Zh. Neorg. Khim.* **1993**, *38*, 1501. (d) Albarski, O.; Hillebrecht, H.; Rotter, H. W.; Thiele, G. *Z. Anorg. Allg. Chem.* **2000**, *626*, 1296.

- (5) Pakhomov, V. I.; Goryunov, A. V.; Ivanova-Korfini, I. I.; Boguslavskii, A. A.; Lotfullin, R. Sh. *Zh. Neorg. Khim.* **1991**, *36*, 1408.
- (6) Pakhomov, V. I.; Goryunov, A. V. *Zh. Neorg. Khim.* **1994**, *39*, 550.
- (7) Pakhomov, V. I.; Fedorov, P. M.; Sadikov, G. G. *Kristallogr.* **1978**, *23*, 615.
- (8) (a) Semin, G. K.; Alymov, I. M.; Burbelo, V. M.; Pakhomov, V. I.; Fedorov, P. M. *Izv. Akad. Nauk SSSR, Ser. Fiz.* **1978**, *42*, 2095. (b) Pakhomov, V. I.; Fedorova, N. M.; Ivanova-Korfini, I. N. *Koord. Khim.* **1978**, *4*, 1765. (c) Pinheiro, C. B.; Jorio, A.; Pimenta, M. A.; Speziali, N. L. *Acta Crystallogr., Sect. B* **1998**, *54*, 197.
- (9) Walha, S.; Savariault, J. M.; Jaud, J.; Ben Salah, A. *Phys. Chem. News* **2002**, *8*, 69.
- (10) Pakhomov, V. I.; Fedorov, P. M.; Ivanova-Korfini, I. N. *Koord. Khim.* **1979**, *5*, 1245.
- (11) Ben Salah, A.; Bats, J. W.; Kalus, R.; Fuess, H.; Daoud, A. Z. *Anorg. Allg. Chem.* **1982**, *493*, 178.
- (12) Burshtein, I. F.; Poznyak, A. L. *Zh. Strukt. Khim.* **1999**, *40*, 541.
- (13) Goggin, P. L.; King, P.; McEwan, D. M.; Taylor, G. E.; Woodward, P.; Sandstrom, M. J. *Chem. Soc., Dalton Trans.* **1982**, 875.
- (14) Zabel, M.; Poznyak, A. L.; Pavloskii, V. I. *Zh. Neogr. Khim.* **2005**, *50*, 1991.
- (15) Danopoulos, A. A.; Wilkinson, G.; Sweet, T. K. N.; Hursthouse, B. M. J. *Chem. Soc., Dalton Trans.* **1995**, 937.
- (16) Pabst, I.; Sondergeld, P.; Czjzek, M.; Fuess, H. *Z. Naturforsch. B* **1995**, *50*, 66.
- (17) Linden, A.; James, B. D.; Liesegang, J.; Gonis, N. *Acta Crystallogr., Sect. B* **1999**, *55*, 396.
- (18) Ben Salah, A.; Bats, J. W.; Fuess, H.; Daoud, A. *Inorg. Chim. Acta* **1982**, *63*, 169.
- (19) Ben Salah, A.; Bats, J. W.; Fuess, H.; Daoud, A. *Z. Kristallogr., Kristallochem., Kristallogr.* **1983**, *164*, 259.
- (20) Wasserscheid, P.; Welton, T., Eds. *Ionic Liquids in Synthesis*; Wiley-VCH: Weinheim, Germany, 2007.
- (21) Holbrey, J. D.; Visser, A. E.; Spear, S. K.; Reichert, W. M.; Swatloski, R. P.; Broker, G. A.; Rogers, R. D. *Green Chem.* **2003**, *5*, 129.
- (22) Visser, A. E.; Swatloski, R. P.; Reichert, W. M.; Mayton, R.; Sheff, S.; Wierzbicki, A.; Davis, J. H. Jr.; Rogers, R. D. *Environ. Sci. Technol.* **2002**, *36*, 2523.
- (23) Papaiconomou, N.; Lee, J.-M.; Salminen, J.; von Stosch, M.; Prausnitz, J. M. *Ind. Eng. Chem. Res.* **2008**, *47*, 5080.
- (24) Germani, R.; Mancini, M. V.; Savelli, G.; Spreti, N. *Tetrahedron Lett.* **2007**, *48*, 1767.
- (25) Peise, O.; Ji, L.; Thiel, S. W.; Pinto, N. G. *Main Group Chem.* **2008**, *7*, 181.
- (26) Ji, L.; Thiel, S. W.; Pinto, N. G. *Water, Air, Soil Pollut.: Focus* **2008**, *8*, 349.
- (27) (a) Deng, N.; Li, M.; de Rooy, S. L.; El-Zahab, B.; Warner, I. M. *ECS Trans.* **2010**, *32*, 73. (b) Kogelnig, D.; Stojanovic, A.; von der Kammer, F.; Terzieff, P.; Galanski, M.; Jirsa, F.; Krachler, R.; Hofmann, T.; Keppler, B. K. *Inorg. Chem. Commun.* **2010**, *13*, 1485. (c) Peppel, T.; Köckerling, M.; Geppert-Rybczynska, M.; Ralys, R. V.; Lehmann, J. K.; Verevkin, S. P.; Heintz, A. *Angew. Chem., Int. Ed.* **2010**, *49*, 7116. (d) Krieger, B. M.; Lee, H. Y.; Emge, T. J.; Wishart, J. F.; Castner, E. W. Jr. *Phys. Chem. Chem. Phys.* **2010**, *12*, 8919. (e) Yoshida, Y.; Saito, G. *Phys. Chem. Chem. Phys.* **2010**, *12*, 1675. (f) Li, M.; De Rooy, S. L.; Bwambok, D. K.; El-Zahab, B.; DiTusa, J. F.; Warner, I. M. *Chem. Commun.* **2009**, *45*, 6922. (g) Yoshida, Y.; Tanaka, H.; Saito, G.; Ouahab, L.; Yoshida, H.; Sato, N. *Inorg. Chem.* **2009**, *48*, 9989. (h) Getsis, A.; Balke, B.; Felser, C.; Mudring, A.-V. *Cryst. Growth Des.* **2009**, *9*, 4429. (i) Branco, A.; Branco, L. C.; Pina, F. *Chem. Commun.* **2011**, *47*, 2300. (j) Mallick, B.; Balke, B.; Felser, C.; Mudring, A.-V. *Angew. Chem., Int. Ed.* **2008**, *120*, 7635.
- (28) (a) Arenz, S.; Babai, A.; Binnemans, K.; Driesen, K.; Giernoth, R.; Mudring, A.-V.; Nockemann, P. *Chem. Phys. Lett.* **2005**, *402*, 75. (b) Mudring, A.-V.; Babai, A.; Arenz, S.; Giernoth, R.; Binnemans, K.; Driesen, K.; Nockemann, P. *J. Alloys Compd.* **2006**, *418*, 204. (c) Babai, A.; Mudring, A.-V. *Chem. Mater.* **2005**, *17*, 6230. (d) Tang, S.-F.; Babai, A.; Mudring, A.-V. *Angew. Chem., Int. Ed.* **2008**, *120*, 7631.

- (e) Tang, S.; Mudring, A.-V. *Eur. J. Inorg. Chem.* **2009**, *19*, 2769.
(f) Mudring, A.-V.; Tang, S. F. *Eur. J. Inorg. Chem.* **2010**, 2569.
(29) Brown, R. J. C.; Dyson, P. J.; Ellis, D. J.; Welton, T. *Chem. Commun.* **2001**, 1862.
(30) (a) Abbott, A. P.; Capper, G.; Davies, D. L.; Munro, H. L.; Rasheed, R. K.; Tambyrajah, V. *Chem. Commun.* **2001**, 1862.
(b) Abbott, A. P.; Capper, G.; Davies, D. L.; Rasheed, R. *Inorg. Chem.* **2004**, *43*, 3447. (c) Zhong, Ch.; Sasaki, T.; Jimbo-Kobayashi, A.; Fujiwara, E.; Kobayashi, A.; Tada, M.; Iwasawa, Y. *Bull. Chem. Soc. Jpn.* **2007**, *80*, 2365. (d) Hitchcock, P. B.; Lewis, R. J.; Welton, T. *Polyhedron* **1993**, *12*, 2039. (e) Hitchcock, P. B.; Seddon, K. R.; Welton, T. *J. Chem. Soc., Dalton Trans.* **1993**, 2639. (f) Hasan, M.; Kozhshen'nikov, I. V.; Siddiqui, M. R. H.; Femoni, C.; Steiner, A.; Winterton, N. *Inorg. Chem.* **1999**, *38*, 5637. (g) Hasan, M.; Kozhshen'nikov, I. V.; Siddiqui, M. R. H.; Femoni, C.; Steiner, A.; Winterton, N. *Inorg. Chem.* **2001**, *40*, 795. (h) Saha, S.; Hayashi, S.; Kobayashi, A.; Hamaguchi, H. *Chem. Lett.* **2003**, *32*, 740. (i) Holbrey, J. D.; Reichert, W. M.; Nieuwenhuysen, M.; Johnston, S.; Seddon, K. R.; Rogers, R. D. *Chem. Commun.* **2003**, 1636. (j) Katayama, Y.; Konishiikem, I.; Miura, T.; Kishi, T. *J. Power Sources* **2002**, *109*, 327. (k) Xu, W.; Copper, E. I.; Angell, C. A. *J. Phys. Chem. B* **2003**, *107*, 6170.
(31) (a) Pyykkö, P. *Chem. Rev.* **1988**, *88*, 563. (b) Mudring, A.-V.; Jansen, M. *Angew. Chem., Int. Ed.* **2000**, *39*, 3066. (c) Mudring, A.-V.; Nuss, J.; Wedig, U.; Ramalho, J. P.; Romero, A. H.; Parrinello, M.; Wagner, F. E.; Krämer, S.; Mehring, M.; Jansen, M. *Angew. Chem., Int. Ed.* **2002**, *41*, 120. (d) Thayer, J. S. *J. Chem. Educ.* **2005**, *82*, 1721. (e) Schwerdtfeger, P.; Bast, R.; Gerry, M. C. L.; Jacob, C.; Jansen, M.; Kellö, V.; Mudring, A.-V.; Saue, T.; Söhnel, T.; Wagner, F. E. *J. Chem. Phys.* **2005**, *122*, 124317. (f) Biering, S.; Hermann, A.; Furthmüller, J.; Schwerdtfeger, P. *J. Phys. Chem. A* **2009**, *113*, 12427. (g) Meyer, G.; Nockemann, P. *Z. Anorg. Allg. Chem.* **2003**, *629*, 1447.
(32) Jander, G.; Brodersen, K. *Z. Anorg. Chem.* **1950**, *262*, 33.
(33) Cutforth, B. D.; Gillespie, R. J. *Inorg. Synth.* **1979**, *19*, 22.
(34) Dupont, J.; Consorti, C. S.; Suarez, P. A. Z.; de Souza, R. F. *Org. Synth.* **2003**, *79*, 236.
(35) *X-Red*; Stoe & Cie: Darmstadt, Germany, 2002.
(36) *X-Shape*; Stoe & Cie: Darmstadt, Germany, 2002.
(37) Sheldrick W. S. *SHELXS-97*: Universität Göttingen: Göttingen, Germany, 1997.
(38) Prince, E., Ed. *International Table for Crystallography*; Kluwer Academic Publishers: Dordrecht, The Netherlands, 2004; Vol. C.
(39) *Diamond*, version 3.2; Crystal Impact GbR; Bonn, Germany, 2010.
(40) Subramanian, V.; Seff, K. *Acta Crystallogr., Sect. B* **1980**, *36*, 2132.
(41) Fenn, R. H. *Acta Crystallogr.* **1966**, *20*, 20.
(42) Harris, G. S.; Inglis, F.; McKechnie, J.; Cheung, K. K.; Ferguson, G. *Chem. Commun.* **1967**, 442.
(43) (a) Babai, A.; Mudring, A.-V. *Acta Crystallogr.* **2005**, *E61*, o1534. (b) Getsis, A.; Mudring, A.-V. *Acta Crystallogr.* **2005**, *E61*, o2945. (c) Babai, A.; Mudring, A.-V. *Z. Anorg. Allg. Chem.* **2008**, *634*, 938. (d) Mallick, B.; Balke, B.; Felser, C.; Mudring, A.-V. *J. Am. Chem. Soc.* **2008**, *130*, 10068. (e) Getsis, A.; Mudring, A.-V. *Cryst. Res. Technol.* **2008**, *43*, 1187.
(44) Steiner, T. *Acta Crystallogr.* **1998**, *B54*, 456.
(45) (a) Barr, R. M.; Goldstein, M. J. *Chem. Soc., Dalton Trans.* **1974**, 1180. (b) Barr, R. M.; Goldstein, M. J. *Chem. Soc., Dalton Trans.* **1976**, 1593.
(46) Mudring, A.-V. *Aust. J. Chem.* **2010**, *63*, 544.
(47) Bard, A. J.; Parsons, R.; Jordan, J. *Standard Potentials in Aqueous Solutions*; Marcel Dekker: New York, 1985.